



Bounded Interval Fuzzy Control for Half Vehicle's Active Suspension System

Rami AL-Jarrah, Hitham Tlilan, Ayat Al-Jarrah

Abstract: A novel efficient control scheme for an active vehicle suspension system is to be designed and simulated in this paper. A half car model has been designed and controlled using two different schemes of standard fuzzy control and bounded interval fuzzy control using MATLAB/SIMULINK. The bounded interval fuzzy control is designed to reduce the uncertainties in the fuzzy sets system and solve the non-linear control problem that the standard fuzzy control cannot handle it. It should be noted that fuzzy logic system is capable of dealing with imprecise concepts and numerous vague but the design of membership functions is nontrivial task. This is because of uncertainty degree that is caused due to road inputs profiles, fuzzy knowledge rules and immeasurable disturbance. The proposed method is expected to be able to mimic the heuristic knowledge of design the membership functions which depends on degree of uncertainty. The membership functions will be generated online during the process in order to deal with uncertainties. The simulation results have demonstrated that the proposed control exhibits better performance and stability as compared to standard fuzzy logic. In addition, the proposed scheme presents a preferable solution and balancing achievement between ride comfort and handling performance. These results demonstrated that the body accelerations and tire dynamic loads will be reduced for the vehicle suspension system in either automobiles or robotics suspension systems.

Keywords: Vibrations; suspension system; fuzzy control; degree of uncertainty

Nomenclature

M_{HCar}	body mass is sprung mass of vehicle
I	body moment of inertia about y-axis
K_3	front suspension stiffness
K_1	rear suspension stiffness
M_{tf}	Front unsprung mass
M_{tr}	Rear unsprung mass
K_4	Front wheel stiffness
K_2	Rear wheel stiffness
b_3	front suspension damping
b_1	rear suspension damping
b_2	Rear wheel damping
b_4	Front wheel damping

θ	the vehicle's pitch angle
a	longitudinal distance of front wheel center to gravity of body center
b	longitudinal distance of rear wheel center to gravity of body center
R_1	road elevation of front tires
R_2	road elevation of rear tires
F_f	actuator force for front suspension system
F_r	actuator force for rear suspension system
$F_q(n)$	The road displacement m^2/m^{-1}
$F_q(n_0)$	Road surface in ISO classification
n	Space frequency
$n_0=0.1m$	Reference space frequency
$w = 2$	Linear fitting coefficient
v	Vehicle speed
f	Time frequency
Ω	angular spatial frequency, W [rad/m]
α	Variable depends on the type of road surface.
$r_0(t)$	Random exciting function, here it is a Gaussian white noise with variance $\sigma=0.1$
$R_0(t)$	The road input displacement function
$h(t)$	Real even function
$h(f)$	Fourier Transform for real even functions
$F_q(n)$	The road displacement
$F_q(n_0)$	Road surface with 8 in ISO classification
n	Space frequency
$n_0=0.1/m$	Reference space frequency
$\mu(x)$	membership functions
δ_L^a	Left bounded values in breakpoint a
δ_R^a	Right bounded values in breakpoint a
δ_L^d	Left bounded values in breakpoint d
δ_R^d	Right bounded values in breakpoint d

I. INTRODUCTION

The vehicle suspension system is playing very crucial role in vehicle because it supports the vehicle body and it provides a ride comfort by decreasing the vibrations. The comfortable ride and the road handling can be measured by observing the body acceleration and suspension deflection, respectively. The suspension system can be categorized to three main categories, namely, passive, semi active and active suspension systems. Despite that the passive suspension via a damper has the ability to store energy and dissipate it; it could only achieve either a ride comfort or a road handling. This is because these two criteria are conflicting with each other and they comprise variations in the spring and damper characteristics.

Manuscript published on 30 September 2019

* Correspondence Author

Rami AL-Jarrah*, Mechanical Engineering Department, Hashemite University, PO. Box 330127, Zarqa 13133, Jordan. Email: ramia@hu.edu.jo

Hitham Tlilan, Mechanical Engineering Department, Hashemite University, PO.Box330127, Zarqa 13133, Jordan. Email: hitham@hu.edu.jo

Ayat Al-Jarrah, Mechatronics Engineering Department, Hashemite University, Zarqa, Jordan. Email: [AyatAljarrah@hu.edu.jo](mailto:ayat@jarrah@hu.edu.jo)

© The Authors. Published by Blue Eyes Intelligence Engineering and Sciences Publication (BEIESP). This is an open access article under the CC-BY-NC-ND license <http://creativecommons.org/licenses/by-nc-nd/4.0/>

On the other hand, the semi-active suspension system provides considerable improvement due to its variable damping characteristics and low power consuming.

Some researchers concentrate on the smart damping technology by employing semi-active system with equivalent performance to active suspension system [1]. There are several suspension systems forms, but the active suspension system is the most accepted one. This is due to the fact that its control system will achieve the performance improvement effectively when comparing to passive or semi-active suspension systems [2, 3]. Moreover, researchers recently are focusing on building the model that is guaranteed the stability as well as designing a control system that is improved the performance of the suspension system. As a result, many models of vehicle suspension systems and control strategies have been proposed [4-8]. Because the vehicle model is very important for researchers in order to control the suspension system, many researches have been introduced based on quarter-car, half-car and full-car suspension models [9-13].

Different control strategies, either classical or intelligent, for the active suspension system have been reported for several researches. The powerful tools of fuzzy model, which is an important branch of intelligent control, are used to handle the uncertainties in the uncertain active suspension systems [14, 15]. The fuzzy logic control (FLC) for active suspension systems is very popular used for improving the road handling and ride comfort and it has been successfully employed for both theoretical and practical systems. It has been found that FLC gives higher robust and better performance comparing to conventional PID and linear quadratic regulator (LQR) controllers [16, 17]. In [18], the PID and FLC for 8 DOF quarter car model was presented and the obtained results showed that FLC has much better ride quality than either PID or passive system. In [19], the authors presented the particles swarm optimization (PSO) that is used to design FLC and its membership functions (MSF) to control active suspension system for a quarter car model. However, this algorithm was carried out in a simple manner and specialized to find out only the centers of output MSF without dealing with the inputs MSF and the obtained results are only compared with passive suspension system model. Although the fuzzy systems give good performances for specific applications under certain particular properties, but under the general fuzzy framework it has some kind of drawbacks and uncertainties which are not easy to handle [20-23].

The design of active suspension system using fuzzy control requires an intelligent behavior with some degree of uncertainty. This degree of uncertainty, which occurs due to missing, imprecise, or unavailable of data, plays a critical role in the development of such knowledge based system. Even though the fuzzy logic system is capable of dealing with imprecise concepts and numerous vague, but the design of membership functions is nontrivial task. The chosen method which is able to mimic the heuristic knowledge of design the membership functions depends on the complexity of the nature of that uncertainty as well as the available data to support the probabilities of such uncertainty. In the vehicle suspension system the uncertainty might come into the control system from many resources such as the random road surfaces and changing in the environmental conditions. In addition,

some uncertainties might be occurred due to MSF and fuzzy rules because different fuzzy rules and MSF will yield to different results [24-27]. Some researchers were proposed two layers fuzzy system which is similar to the neural network in the shape but it does not form the neural nodes [28, 29]. However, the time process of these kinds of fuzzy systems has a large computational cost. The type-2 FLC (T2FLC) system was presented to model the uncertainties in fuzzy systems and to improve the capability of the fuzzy system [30-32]. The T2FLC was presented in [32] to deal with system time-varying and the uncertain behaviors to reduce the vehicle vibrations and increase the performance. However, the defuzzification process time for T2FLC systems has a large computational cost. Whilst non-stochastic uncertainties in practical applications were handled by T2FLC, the traditional fuzzy is not the best choice to deal with stochastic uncertainties [32]. However, these uncertainties, sometimes called noise, might arise in the information either during the collected time or the processed time [33]. The probabilistic fuzzy logic system (PFLS) was proposed instead of the standard fuzzy set to deal with the stochastic uncertainties information [34, 35]. PFLS is different than FLC since it uses probabilistic fuzzy sets rather than fuzzy sets to reduce the information with stochastic uncertainties. It can handle the computing time by introduced new methods and algorithms based on integrating the probabilistic information into MSF. In addition, The PFLS was not only able to handle uncertainties in complex plant dynamics, but also it has the ability to improve the performance and reasoning in the unknown dynamic environments [35]. However, in order to quantify uncertainty, PFLS needs to repeat the measurement for several times to estimate the value and its standard deviation. In addition, the changing in the suspension vehicle environment conditions and the random road profiles as well as the understanding of the fuzzy knowledge based and linguistics variables have led to not able to solve all the uncertainties problems. These difficulties to deal with all problems make it hard to design proper fuzzy control system.

Thus, this paper aims to propose a powerful and potential controller that is capable of handling linguistic uncertainty by either understanding of linguistic knowledge or quantification of fuzzy rules. Also, design a fuzzy controller that is superior to existing controllers. Therefore, in this paper, a bounded interval fuzzy control (BIFC) is presented for a half vehicle active suspension system. By implementing the uncertainties degree in the MSF, the performance of the proposed fuzzy system to reduce the disturbance is increased effectively. In addition, the algorithm has ability to optimize the initial MSF online during the process. The BIFC is similar to the standard fuzzy control by containing main stages such as fuzzification, inference systems, and defuzzification. However, the proposed approach stages have different operation methods. The reminder of this paper is organized as follows: after the introduction section we will discuss the model of the half vehicle dynamic system in Section 2. Section 3 presents the proposed fuzzy controller. The results are presented in section 4. Finally, section 5 presents the conclusion of the work.

II. MODELING OF HALF VEHICLE DYNAMIC

Indeed, compromising between vehicle dynamics and the simplicity is very important criterion in modeling the system to have a balance between the accuracy and efficiency. Even though the quarter car model has the simplest construction, but unfortunately it has the lowest degree of freedom (DOF). Then, the vehicle dynamic couldn't be realized in a good manner. On the contrary, the full car suspension model is capable of realizing the vehicle dynamics because it has the highest DOF. Thus, active vehicle suspension is presented by using half-vehicle model to achieve this compromising as it is shown in Fig. 1. Two actuators are presented at front and rear suspensions to achieve ride comfort and to improve ride quality. In Fig. 1, the displacements of front vehicle body, front tire, rear vehicle body and rear tire measured with respect to position of equilibrium are X_{f1} , X_{f2} , X_{r1} , and X_{r2} respectively.

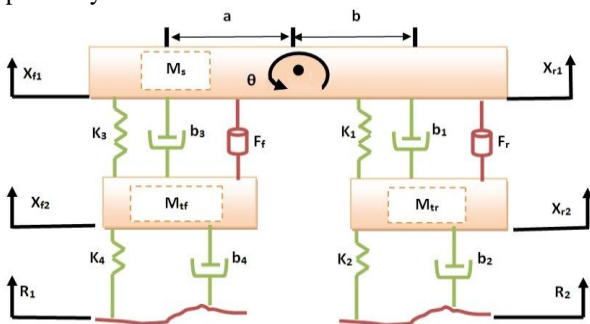


Fig. 1. The half Vehicle model

The selected parameters of the active suspension are given in Table I. The changing of the vehicle's properties and parameters will not affect the proposed fuzzy control performance. The dynamic equations of motion are shown in equation (1) to equation (4).

$$\ddot{X}_{f1} = F_f + b_3(\dot{X}_{f2} - \dot{X}_{f1}) + k_3(X_{f2} - X_{f1}) \left(\frac{1}{M_{HCar}} + \frac{a^2}{I} \right) + F_r + b_1(\dot{X}_{r2} - \dot{X}_{r1}) + k_1(X_{r2} - X_{r1}) \left(\frac{1}{M_{HCar}} - \frac{ab}{I} \right) \quad (1)$$

$$\ddot{X}_{r1} = F_f + b_3(\dot{X}_{f2} - \dot{X}_{f1}) + k_3(X_{f2} - X_{f1}) \left(\frac{1}{M_{HCar}} + \frac{ab}{I} \right) + F_r + b_1(\dot{X}_{r2} - \dot{X}_{r1}) + k_1(X_{r2} - X_{r1}) \left(\frac{1}{M_{HCar}} - \frac{b^2}{I} \right) \quad (2)$$

$$\ddot{X}_{f2} = \frac{-1}{M_{tf}} \left[F_f + b_3(\dot{X}_{f2} - \dot{X}_{f1}) + k_3(X_{f2} - X_{f1}) + k_4(X_{f2} - R_1) + b_4(\dot{X}_{f2} - \dot{R}_1) \right] \quad (3)$$

$$\ddot{X}_{r2} = \frac{-1}{M_{tr}} \left[F_r + b_1(\dot{X}_{r2} - \dot{X}_{r1}) + k_1(X_{r2} - X_{r1}) + k_2(X_{r2} - R_2) + b_2(\dot{X}_{r2} - \dot{R}_2) \right] \quad (4)$$

Table I. Half vehicle properties

Parameters	Value
a	1.4 m
b	1.3 m
MHCar	803 kg

I	3128(kg m ²)
K3	130000(N/m)
K1	85000(N/m)
Mtf	90 kg
Mtr	115 kg
K4	405000 (N/m)
K2	405000 (N/m)
b3	3040(N-sec/m)
b1	3040 (N-sec/m)
b2	70 (N-sec/m)
b4	80 (N-sec/m)

A. Model of road input profile

Three road profiles have been used in order to examine the performance of the proposed control. The step input, sine wave as well as random road profiles surfaces are being used to obtain the system response and performance. Therefore, the step input will characterize a sudden change of the road surface for either a pothole with a depth of 10cm or a 10cm bump. In the sine wave bump, it has been assumed that the road profile approximated by a sine wave with amplitude= 0.1m as it is shown in Fig.2.

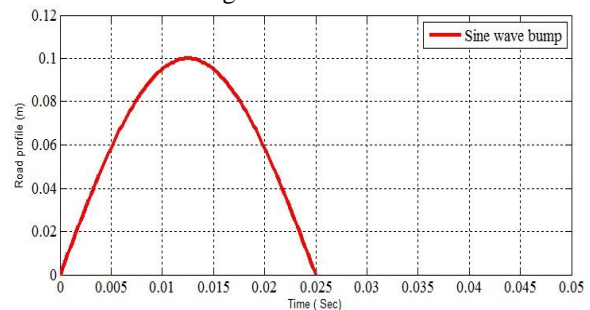


Fig. 2. The sine wave bump

However, to precisely demonstrate the performance of an active suspension system, a perfect model for the natural changing conditions is important while designing the control system. Whilst the simple functions such as sine waves and step input are easily to apply as road inputs, but they are not ideal representation for practical applications. Thus, the deterministic shapes are not validity for studying the actual behavior. Meanwhile, the Power Spectral Density (PSD) theory gives capability to describe the road surface as a random exciting function. In addition, the roughness classification of the road surfaces according to ISO as it is illustrated in Table II. The random road surface can be designed as it is illustrated in Fig.3.

Table II. Road roughness value by ISO [36, 37, 38].

Road	Class	Roughness degree $\phi(n_0)$ [$10^{-6}m^2/$ (cycle/m)]	Roughness degree $\phi(\Omega_0)$ ($10^{-6}m^3$ where $\Omega_0 = 1rad/m$)
Good	B	64	4
Average	C	256	16
Poor	D	1,024	64
Very poor	E	4,096	256

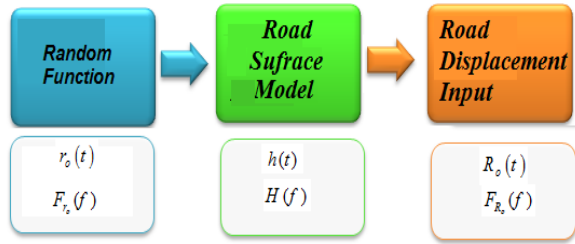


Fig. 3. The model for random road surface

The random road profile by PSD [39] can be chosen in the spatial frequency as

$$\Phi(\Omega) = \frac{2\alpha \times 4 \times \Phi(\Omega_o)}{\Omega_o^2 + \alpha^2} \quad (5)$$

Thus; $\alpha=0.127$ and for the other road classes, the road class standard deviations could be found in Table III. In appendix B, one can find more details about the random road profile by PSD.

Table III. Standard deviation of road class[39]

Class	Standard deviation	$\Phi(\Omega_o)$	α
B	0.004	4	0.127
C	0.008	16	0.127
D	0.016	64	0.127
E	0.032	256	0.127

III. DESIGN OF BOUNDED INTERVAL FUZZY CONTROL (BIFC)

In this section, the design of adaptive fuzzy control with bounded intervals membership functions will present.

A. Design the Fuzzy sets system:

Although the standard fuzzy logic system is capable of mapping the input-output relation of a model without a mathematical model, but it does may not be able to handle the uncertainties in any practical applications [34, 35]. The main uncertainties in standard fuzzy logic can be occurred due to inputs variability and designing of linguistic fuzzy knowledge and rules. However, the degree of uncertainty can be introduced to define the uncertainty margin in the membership functions $\mu(x)$; then; an adaptive fuzzy system can be proposed to design the proper membership functions for suspension system. Moreover, all membership functions could be described by α -cut ($A\alpha = x | \mu(x) \geq \alpha$ and $\alpha \in \{0, 1\}$). As it is common that all α -cuts are intervals $A\alpha = \{x1(\alpha), x2(\alpha)\}$. The educing and interpolation is usually performed in terms of α -cut. For instance, the educing of the two intervals $A0 = \{x1, x2\}$ and $A1 = \{x3, x4\}$ could be easy to interpolated to arbitrary α . Regarding to mathematical viewpoint, the trapezoidal membership functions is working well in real time applications. This is because the linear interpolation is used to find the endpoints of the interval $A\alpha$: $A\alpha = \{\alpha \cdot x3 + (1 - \alpha) \cdot x1, \alpha \cdot x4 + (1 - \alpha) \cdot x3\}$. The standard trapezoidal membership function is illustrated in Fig. 4. The $\{a, b, c, \text{ and } d\}$ are the breakpoints and the grade of the membership functions of crisp input $x1$ is μ_0 . The standard trapezoidal membership function, i th is the rules and j th is the input variables, is given by equation (7). However, the trapezoidal membership functions have degree of uncertainties. In regarding to Fig.5, the original membership function belongs to four possible

bounded regions. Here, δ_R and δ_L are defined as right and left bounded uncertainty values in MSF and they will be tuned to create new two sides for the membership functions as it is illustrated in Table IV. Then, the new fuzzy membership function can be given as equation (8). The proposed fuzzy system has the same operations as in the standard system logic such as fuzzification, fuzzy inference system, and defuzzification. However, the new membership functions were generated based on the four uncertainty boundary regions. Meanwhile, the proposed system consists of left fuzzy inference system and right fuzzy inference system which use the max–min product to operate the rules and to reduce the computational time during the process. In addition, they perform the reasoning process with the same fuzzy knowledge rules. The fuzzification process, which has predefined values of the uncertainty, is illustrated in Fig. 6.

$$\mu_{A^{ij}}(x_j) = \begin{cases} \frac{x_j - a_{ij}}{b_{ij} - a_{ij}} & \text{if } a_{ij} \leq x_j \leq b_{ij} \\ 1 & \text{if } b_{ij} \leq x_j \leq c_{ij} \\ \frac{d_{ij} - x_j}{d_{ij} - c_{ij}} & \text{if } c_{ij} \leq x_j \leq d_{ij} \\ 0 & \text{Otherwise} \end{cases} \quad (6)$$

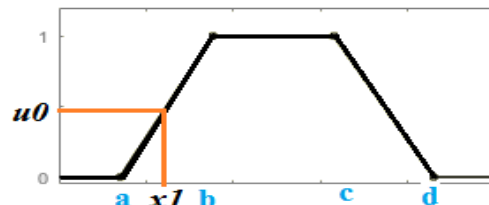


Fig. 4. Trapezoidal fuzzy membership functions.

Table IV. The membership functions

Uncertain values	New break point	$\mu(x1)$
δ_L^a	$a^* = a - \delta_L^a$	$\mu_{\delta_L^a}$
δ_R^a	$a^* = a + \delta_R^a$	$\mu_{\delta_R^a}$
δ_L^d	$d^* = d - \delta_L^d$	$\mu_{\delta_L^d}$
δ_R^d	$d^* = d + \delta_R^d$	$\mu_{\delta_R^d}$

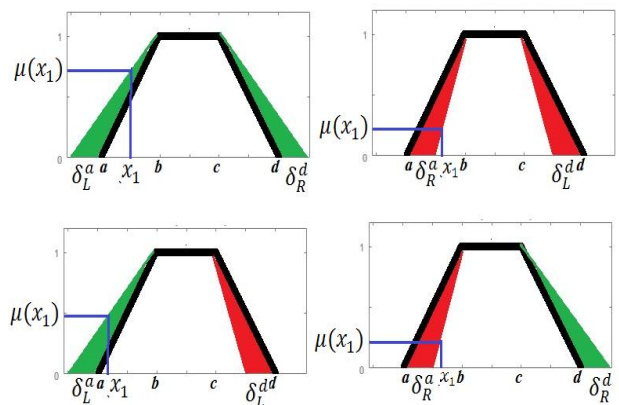


Fig. 5. Uncertainty intervals in trapezoidal MSF.

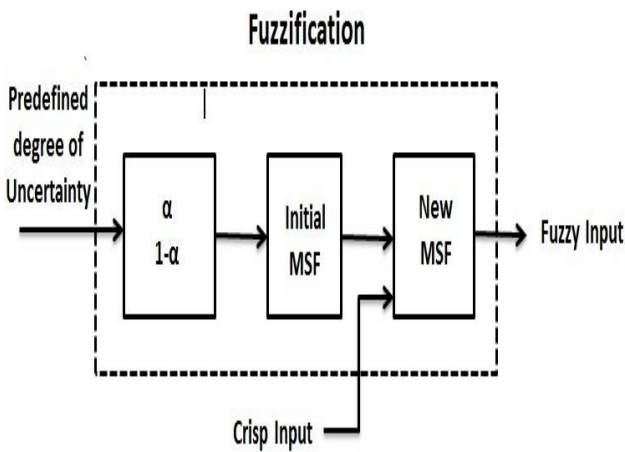


Fig. 6. Fuzzification process

$$\mu_A^{ij}(x_j) = \begin{cases} 0 & x \leq a - \delta_L^a \\ \frac{x - a + \delta_L^a}{b - a + \delta_{L1}^a} & a - \delta_L^a \leq x \leq a \\ \left[\frac{x - a + \delta_L^a}{b - a + \delta_L^a}, \frac{x - a}{b - a} \right] & a \leq x \leq a + \delta_R^a \\ \left[\frac{x - a}{b - a}, \frac{x - a - \delta_R^a}{b - a - \delta_R^a} \right] & a + \delta_R^a \leq x \leq b \\ 1 & b \leq x \leq c \\ \left[\frac{d - \delta_L^d - x}{d - \delta_L^d - c}, \frac{d - x}{d - c} \right] & c \leq x \leq d - \delta_L^d \\ \left[\frac{d - x}{d - c}, \frac{d + \delta_R^d - x}{d + \delta_R^d - c} \right] & d - \delta_R^d \leq x \leq d \\ \frac{d + \delta_R^d - x}{d + \delta_R^d - c} & d \leq x \leq d + \delta_R^d \\ 0 & d + \delta_R^d \leq x \end{cases} \quad (7)$$

Consider a fuzzy control rule represented by general form:
 $R_j = IF A_i \text{ is } \mu_{ij}^A \text{ THEN } Y_i \text{ is } \mu_j^Y$, where $j = (1, 2, \dots, m)$ that denotes the number of rules, $i = (1, 2, \dots, n)$ that denotes the number of input variables). The right and left interval bounded membership functions will be obtained by the adapted max-min method in the inference engine. The multi antecedents for each rule will be connected by using this adapted method by applying the meet operation. The details in order to find the left bounded of the fired the resulting sets by the max-min method are described in Appendix C. However, the resulting sets for left and right is given as the following:

$$Y_{\delta_L}^i = \max\{Y_1^i, Y_2^i, \dots, Y_j^i\} \quad (8)$$

$$Y_{\delta_R}^i = \max\{Y_1^i, Y_2^i, \dots, Y_j^i\} \quad (9)$$

Therefore, in regarding to the fired resulting rule, the interval of inference system can be explained as

$$Y = [Y_{\delta_R}^i, Y_{\delta_L}^i] \quad (10)$$

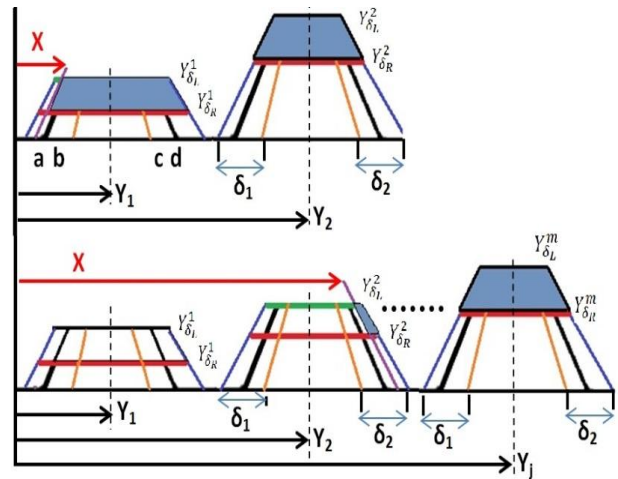


Fig. 7. The weight for left side MSF

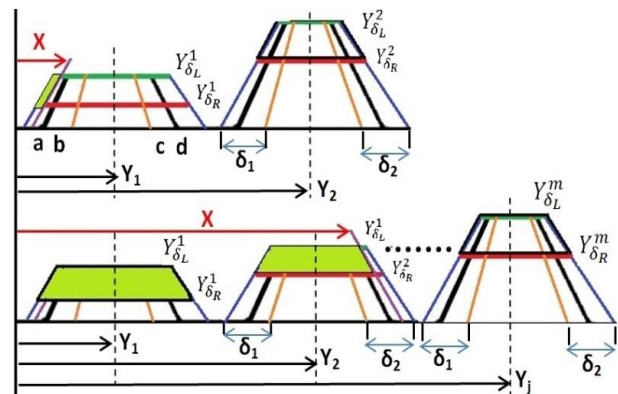


Fig. 8. The weight for right side MSF

The interval of inference system according to equation (10) has two sides the left side and the right one. Rather than using center of gravity for the bounded intervals, the method is determining the weight for each membership function by rearranging the fired intervals. For left and right sides as illustrated in Fig.7 and Fig.8, the left and the right sides points are obtained by the center of gravity method as the following:

$$Y_{\delta_L}^i = \frac{f_1 + f_2 + f_3}{f_1/y^j + 2f_2/(x-a) + f_3/y^j} \quad (11)$$

$$Y_{\delta_R}^i = \frac{f_1 - f_2 - f_3}{f_1/y^j - 2f_2/(x-a) - f_3/y^j} \quad (12)$$

$$f_1 = \left(\delta \sum_{j=1}^m (Y_{\delta_L}^j) y^j \right)$$

$$f_2 = (X - a)(Y_{\delta_L}^k - Y_{\delta_R}^k) \left(\frac{X}{2} - \frac{a}{2} \right) \quad (13)$$

$$f_3 = \sum_{j=1}^m (Y_{\delta_L}^j + Y_{\delta_R}^j - y^j) (Y_{\delta_L}^j - Y_{\delta_R}^j) y^j$$

$$X > a \rightarrow K = j$$

where the point X is a test point that intersects the output membership functions, and y_j is the j th centroid of the output MSF. Next step is the iterations methods which are applied to find and optimize the minimum values of left interval side and right interval side as it is shown in Fig.9 and Fig.10.

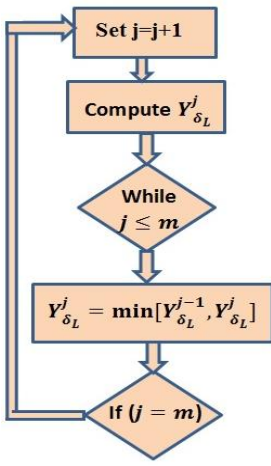


Fig. 9. Iterations method for left interval

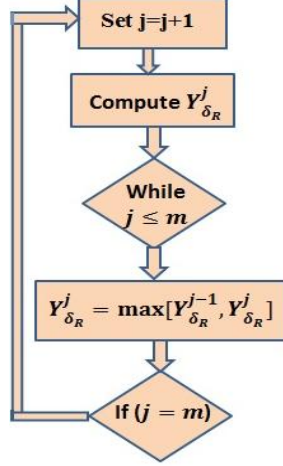


Fig. 10. Iterations method for right interval

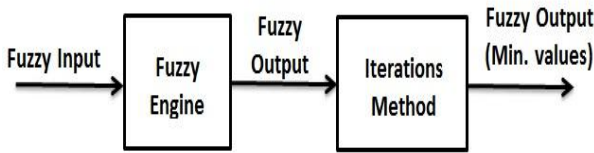


Fig. 11. Fuzzy Engine system

Based on these results (the inference engine results as illustrated in Fig.11, the defuzzification process for the interval of MSF sets is established to derive accurate control system outputs. Thus, the height method and adaptive defuzzification process for the control system with reference function y^{ref} are applied to each interval side as it is shown in Fig. 12. The errors for optimizing the crisp output are describe as

$$e_{\delta_L} = y^{ref} - Y_{\delta_L} \quad (14)$$

$$e_{\delta_R} = y^{ref} - Y_{\delta_R} \quad (15)$$

The degree of the uncertainty based on the height method is given as

$$\alpha = \frac{e_{\delta_R}}{e_{\delta_R} + e_{\delta_L}} \quad (16)$$

$$1 - \alpha = \frac{e_{\delta_L}}{e_{\delta_R} + e_{\delta_L}} \quad (17)$$

The control output y^o is given by

$$y^o = \alpha Y_{\delta_L} + (1 - \alpha) Y_{\delta_R} \quad (18)$$

The tuning process for the degree of uncertainty, which aims to reduce the system error, will be applied to improve the performance of control output. Once left and right sides of degree of uncertainty are tuned to new values, then the new uncertainty bounded regions is rebuilt online during the process in real time.

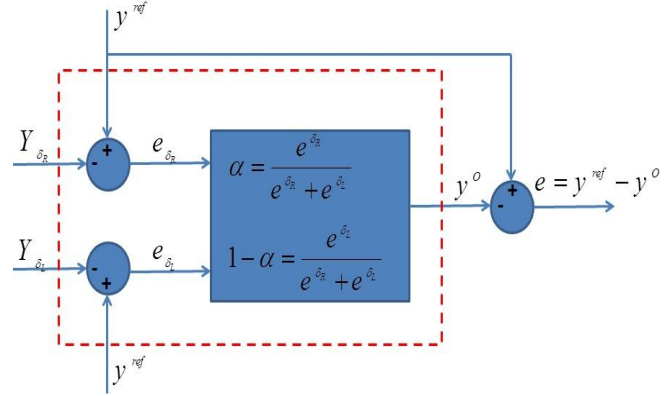


Fig. 12. The adaptive defuzzification process.

B. Fuzzy Control

The proposed fuzzy control system contains three inputs and one output. The first input is the body displacements. The second input is the vehicle body velocities and the pitch angle is chosen as the third input variable. The controller output is the actuator forces. The initial MSF for the three inputs and one output are shown in Table V, Table VI, Table VII and Table VIII, respectively. The number of rules for this controller was 27 base rules as illustrated in Table IX.

Table V. Initial MFs of body displacements

linguistic variables	Initial MSF breakpoints
Negative(N)	{-1000,-1, -0.6, 0}
Zero(Z)	{-0.2, -0.05, 0.05, 0.2}
Positive(P)	{0, 0.6, 1, 1000}

Table VI. Initial MFs of vehicle body velocities

linguistic variables	Initial MSF breakpoints
Negative(N)	{-1000,-1, -0.85, 0}
Zero(Z)	{-0.1, -0.05, 0.05, 0.1}
Positive(P)	{0, 0.85, 1, 1000}

Table VII. Initial MFs of pitch angle

linguistic variables	Initial MSF breakpoints
Negative(N)	{-1000,-1, -0.7, -0.1}
Zero(Z)	{-0.2, -0.04, 0.04, 0.2}
Positive(P)	{0.1, 0.6, 1, 1000}

Table VIII. Initial MFs of control forces

linguistic variables	Initial MSF breakpoints
Negative large (NL)	{-1000,-1, -0.9, -0.4}
Negative small (NS)	{-0.95, -0.55, -0.4, 0}
Zero (Z)	{-0.03, -0.01, 0.01, 0.03}
Positive small (PS)	{0, 0.4, 0.5, 0.95}
Positive large (PL)	{0.4, 0.95, 1, 1000}

Table IX. The fuzzy control rules

Rule	Input 1	Input 2	Input 3	Output
1	N	N	N	PL
2	N	N	Z	PL
3	N	N	P	PL
4	N	Z	N	PS
5	N	Z	Z	PS
6	N	Z	P	PS
7	N	P	N	PS
8	N	P	Z	PS
9	N	P	P	PS
10	Z	N	N	PS
11	Z	N	Z	Z
12	Z	N	P	Z

13	Z	Z	N	Z
14	Z	Z	Z	Z
15	Z	Z	P	Z
16	Z	P	N	NS
17	Z	P	Z	NS
18	Z	P	P	NS
19	P	N	N	NS
20	P	N	Z	NS
21	P	N	P	NS
22	P	Z	N	NS
23	P	Z	Z	NL
24	P	Z	P	NL
25	P	P	N	NL
26	P	P	Z	NL
27	P	P	P	NL

IV. RESULTS

In order to assess the performance of proposed algorithm, the simulations have been carried out on the proposed model system by using MATLAB/Simulink. Moreover, comparing the results between the proposed approach and classical fuzzy control is presented.

A. Step input road profile

For control performance examination, step input bumps road profiles are being used to obtain the system response and performance. Therefore, the step input is employed to describe the situation when the vehicle suddenly crossing over a change of road surface for either a pothole with a bump with a height of 10cm. Fig. 13 and Fig. 14 is illustrated the front and rear body accelerations with both FLC and BIFC controllers, respectively. It is obviously noticed that the proposed BIFC control showing a better ride comfort by decreasing the accelerations and obtaining a smaller settling time in comparing with FLC. According to [40], the dose measurement, which is based on the fourth power of the frequency-weighted acceleration, is superior to using root means square (RMS) for discomfort prediction. Therefore, the vibration dose value (VDV) emphasizes shocks more than the RMS. In addition, VDV does not decay during periods of low vibration magnitude. Furthermore, exposure to continuous vibration will continuously cause VDV to increase while RMS remains constant. Consequently, VDV is recommended above RMS method to evaluate the vehicle ride comfort. The VDV values are calculated in this research and it values are 0.61m/s^{1.75} and 0.48m/s^{1.75}for FLC and BIFC, respectively.

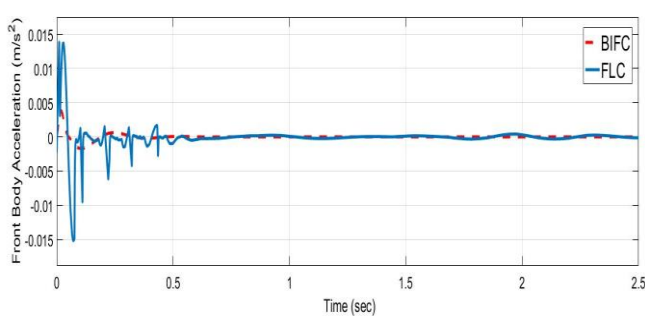


Fig. 13. Front Body acceleration (A)

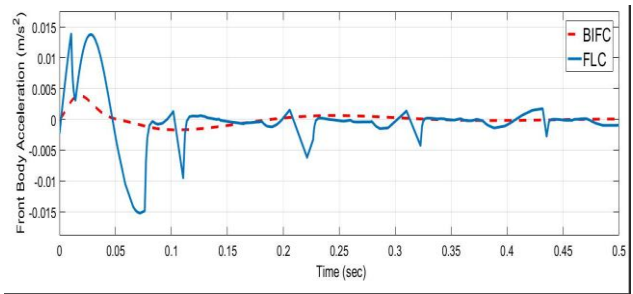


Fig. 13. Enlarged of Front Body acceleration (B).

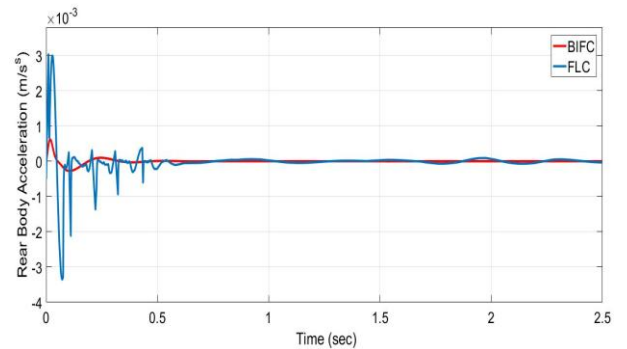


Fig. 14. Rear Body acceleration (A)

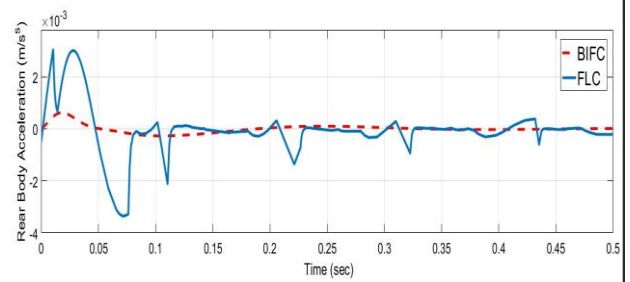


Fig. 14. Enlarged of Rear Body acceleration (B)

Regarding to the vehicle handling performance, the tyre deflection is an important criteria; thus front tyre deflection and rear tyre deflection are shown in Fig. 15 and Fig. 16, respectively. Implemented the fuzzy controller will reduce the deflections significantly. However, it is clear that the proposed method BIFC on comparing to FLC provides minimal deflections of the front and rear tyres. The pitch angle accelerations are illustrated in Fig. 17. In regarding to pitch dynamics output response, the proposed method BIFC has smaller overshoot, smaller settling time and more stability than the FLC method.

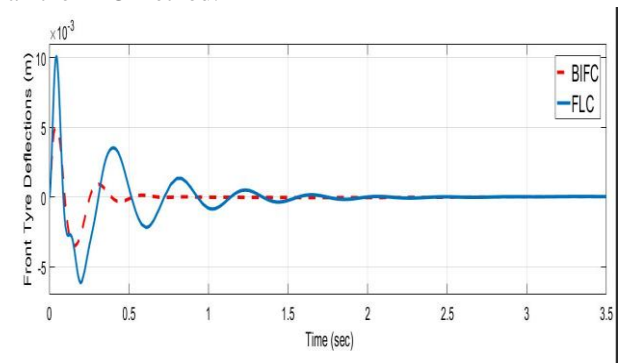


Fig. 15.A. Front tyre deflection

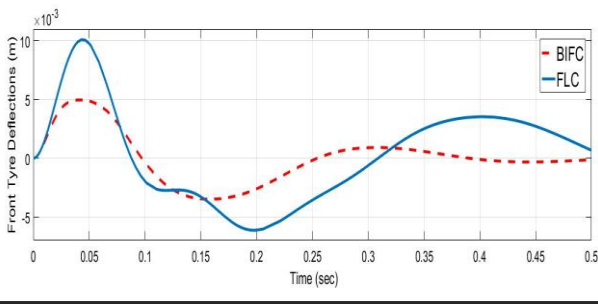


Fig. 15.B. Enlarged of Front tyre deflection

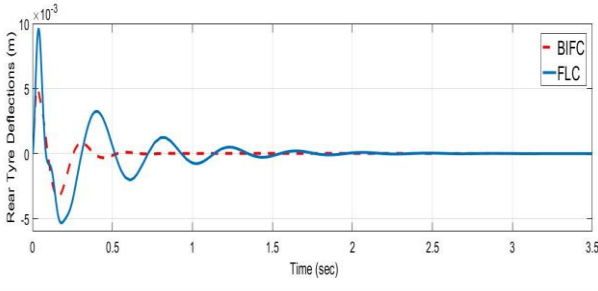


Fig. 16.A. Rear tyre deflection

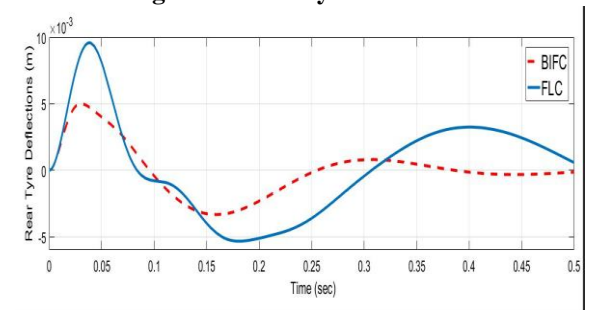


Fig. 16.B. Enlarged of Rear tyre deflection

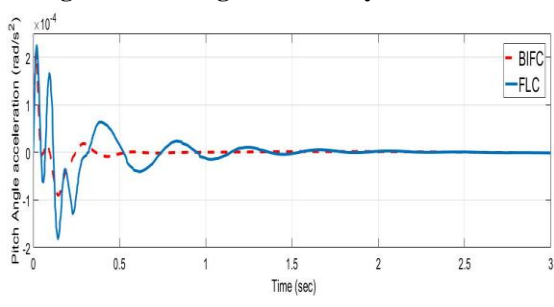


Fig. 17.A. Pitch angle acceleration

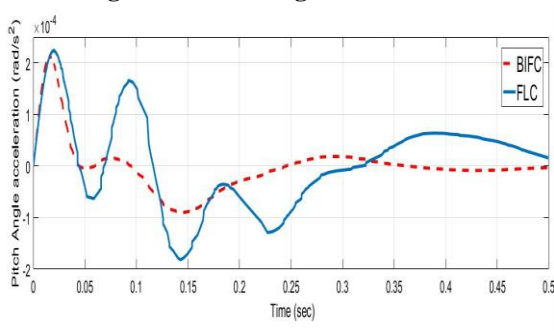


Fig. 17.B. Enlarged Pitch angle acceleration

B. Sine wave road profile

Assuming the road profile approximated by a sine wave bump of amplitude= 0.1m the Fig. 18 and Fig. 19 have shown the front body accelerations and the rear body accelerations, respectively. It is clear that the proposed BIFC control obtains

a better ride comfort by decreasing the accelerations as well as it obtains a smaller settling time comparing to FLC. The VDV's values are 0.65m/s^{1.75} and 0.52m/s^{1.75}for FLC and BIFC, respectively.

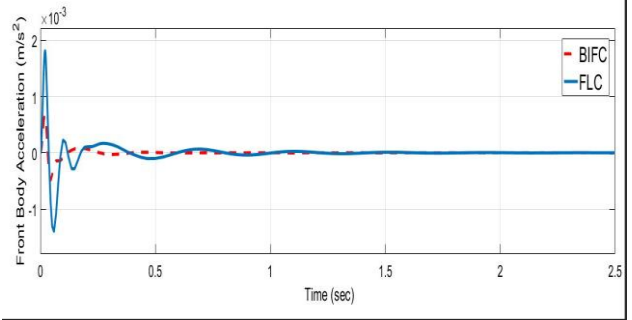


Fig. 18.A. Front body acceleration

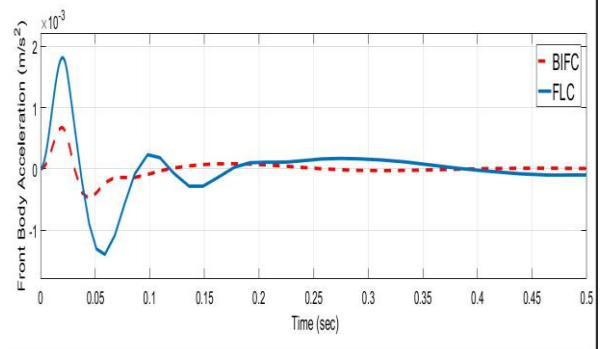


Fig. 18.B. Enlarged of Front body acceleration

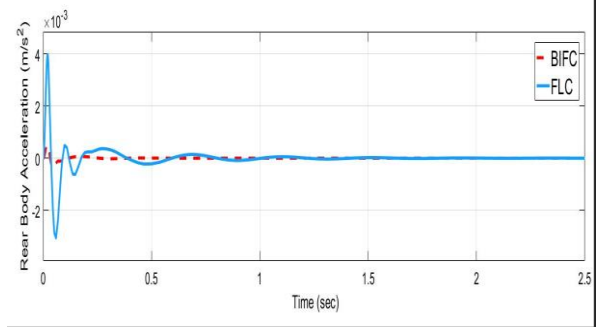


Fig. 19.A. Rear body acceleration

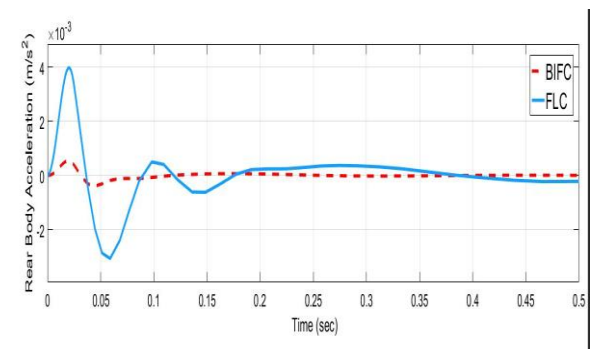


Fig. 19.B. Enlarged of Rear body acceleration

The front tyre deflection and rear tyre deflection are shown in Fig. 20 and Fig. 21, respectively. It is obvious clear that the BIFC provides smaller tyre deflections. The pitch angle accelerations are illustrated in Fig. 22. In regarding to pitch dynamics output response, the proposed method BIFC has smaller overshoot, smaller settling time and more stability than the FLC method.

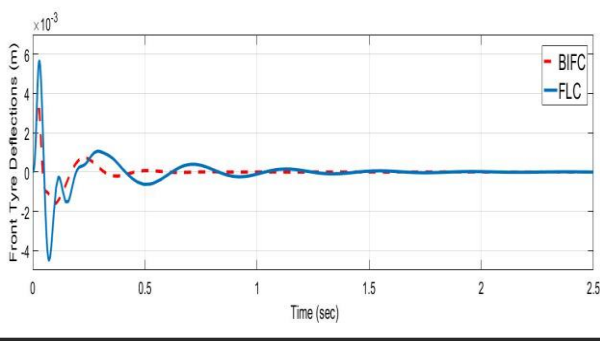


Fig. 20.A. Front tyre deflection

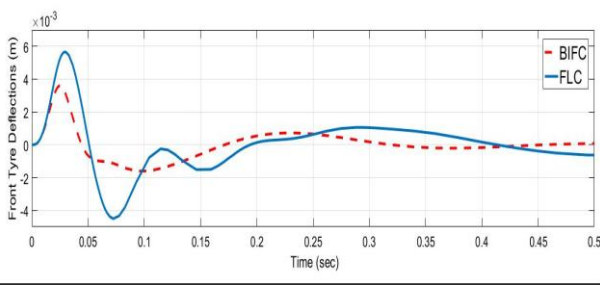


Fig. 20.B. Enlarged of Front tyre deflection

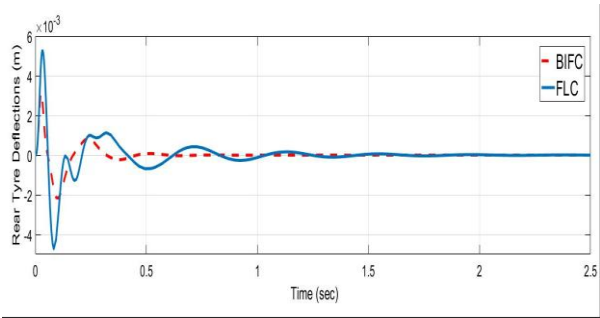


Fig. 21.A. Rear tyre deflection

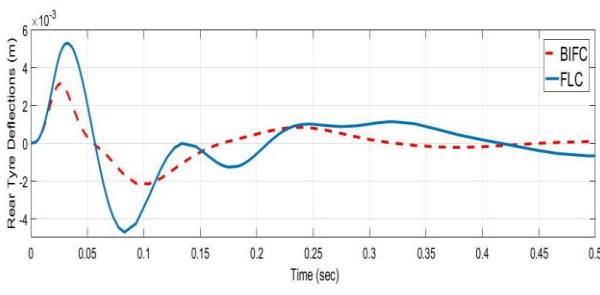


Fig. 21.B. Enlarged of Rear tyre deflection

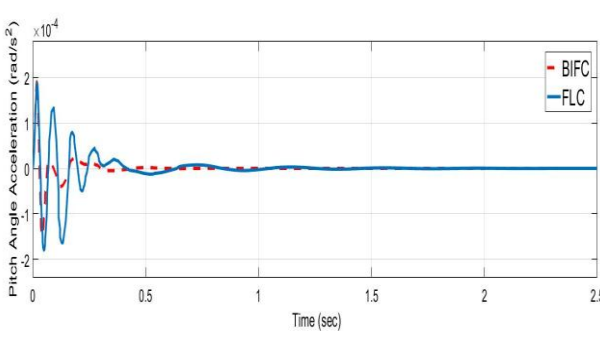


Fig. 22.A. Pitch angle acceleration

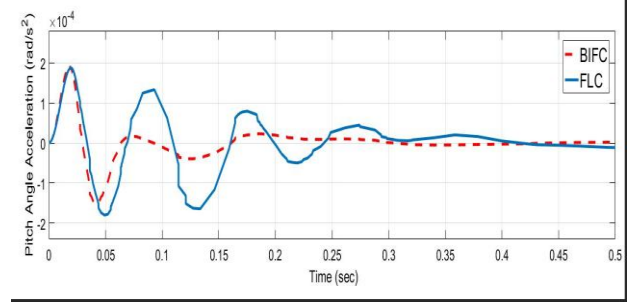


Fig. 22.B. Enlarged of Pitch angle acceleration

C. Random Road input:

The adopted shaping filter method was used to generate the random road profiles for the class of average and poor road as it is shown in Fig. 23. A typical random output of a road profile class B and C generated from the model are shown in Fig. 24 and Fig. 25. The speed of vehicle has been chosen as 16.6m/s.

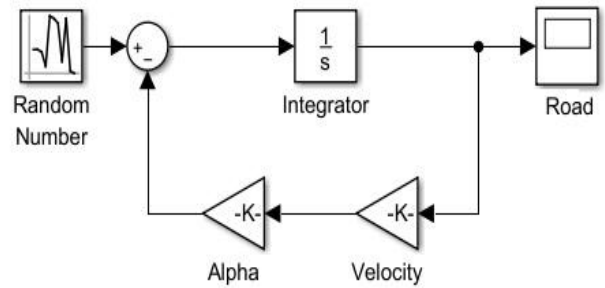


Fig.23 First order linear system

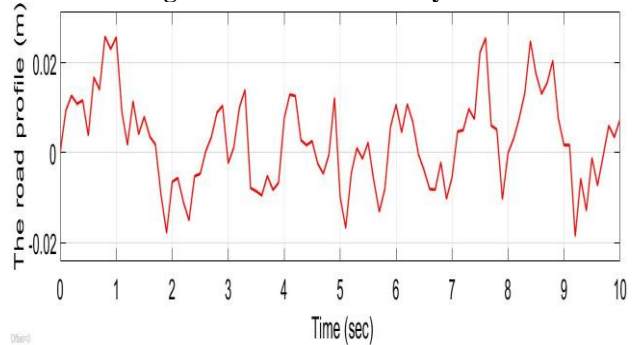


Fig.24 Road profile class B generated from the model.

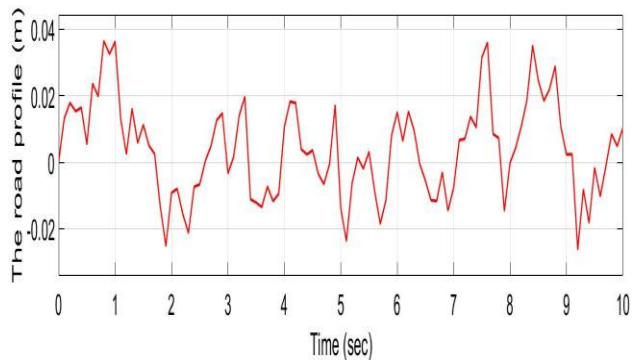


Fig.25 Road profile class C generated from the model.

The performance criterion that is used to evaluate the vehicle suspension system with random road profiles is RMS values. It is capable of evaluating the system from time domain and it presents the compromising between the vehicle ride comforts and handling performance.

In addition, according to the ISO criteria [40], the crest factors which define as a dimensionless quantity as the ratio of the peak acceleration to the RMS is important evaluator of vehicle ride comfort. The comparison of the RMS and peaks values with the normal vehicle mass M_{car} is given in Table X and Table XIII for average and poor road profiles, respectively. When the body mass changes with (-20%), the comparisons results are shown in Table XI and XIV. With +20% changes in the body mass, the RMS values comparisons are given in Tables XI and XVI. Therefore, the RMS values for front body and rear body accelerations are demonstrated that the presented BIFC approach achieved better performance on the ride comfort comparing to FLC. In order to test the robust and adaptive properties of the suspension system with BIFC considers average road profile, the consideration of the sprung mass changes ± 20 percent of nominal values have been implemented as illustrated in Table XVI and XVII. The results show that the proposed method has a superior robust ability and has a preferable solution and balancing achievement between ride comfort and handling performance when the K_1 and K_3 is changed. The crest factors were determined and are given in Table XIX and Table XX for the average and poor road surface, respectively.

Spectral analysis is implemented so check any energy present at any frequency. So for vibration analysis, fast Fourier transform FFT analysis is used to compute the discrete Fourier transform (DFT). This analysis converts time domain to frequency domain. According to ISO 2361, the man body is sensitive to vertical vibrations within frequency range 4-8 Hz [38, 40]. In addition, the comfortable ride is linked to body accelerations frequency response whilst the handling performance is linked to tire dynamic load. Therefore, the frequency response of body acceleration and tire dynamic loads for presented method is shown in Fig. 26 and Fig. 27, respectively. The results are shown that the active suspension has achieved a significant reduction of body accelerations in the frequency 8.9Hz. In addition, at smaller tyre dynamic loads; the handling performance is being improved by the presented approach.

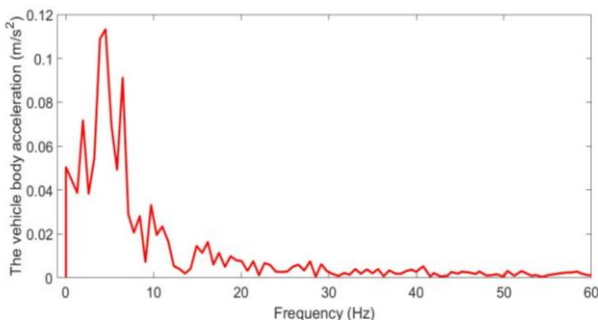


Fig. 26 The frequency response of vehicle body acceleration

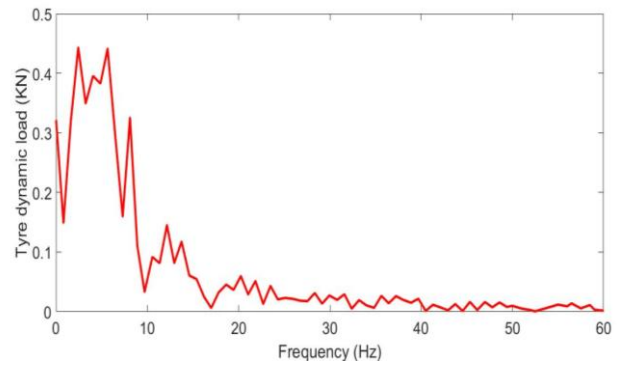


Fig. 27 The frequency response of tyre dynamic load

V. CONCLUSION:

An adaptive fuzzy control scheme with bounded interval membership functions, by using the interval MSF and adaptive optimal strategy, has been presented in this paper.

A systematic methodology is provided to design and control non-linear dynamics and uncertainty in the half-vehicle active suspension system that couldn't be well handled by standard fuzzy control. It has also been validated that the BIFC has the powerful ability to handle uncertainties by either understanding of linguistic knowledge or quantification of fuzzy rules.

Under normal and random roads input profiles, using nominal values of the suspension system as well as with changing these values, the presented controller scheme was presenting a preferable solution and balancing achievement between ride comforts and handling performance.

The vehicle body accelerations and tire dynamic loads were been reducing for the vehicle suspension system by using the proposed control scheme. The vibrations analysis showed that the body accelerations were in the range of the sensitivity of man body to vertical vibrations. Also, at smaller tyre dynamic loads; the handling performance is being improved. In addition, the results convincingly demonstrated that the presented approach can remarkably restrict the vertical vibrations and pitch motion of the vehicle body. The performance criteria that were used to evaluate the vehicle suspension system with random road profiles were RMS and crest factors values. The presented approach presented a good compromising between the vehicle ride comforts and handling performance and the results were in the accepted range.

Future work has aims to address the problem by intelligent computer vision. The performance of the fuzzy image processing system may provide a better estimation of the input road profile and disturbances for either an automobile vehicle or mobile robotics system. In addition, it has been targeted to address the stability of the control and the optimal solutions in MSF. Besides, model of full vehicle is under consideration for future work.

Table X. The comparison of RMS and peak values when the mass = MHcar and road class is average ($\times 10^{-3}$):

		Front body acceleration	Rear body acceleration	Pitch acceleration	Front body deflection	Rear body deflection
FLC	Peak	21.770	4.827	0.2507	13.890	12.470
	RMS	4.923	1.084	0.1121	6.475	5.930
BIFC	Peak	2.304	0.3680	0.1671	6.473	5.954
	RMS	1.078	0.1720	0.1091	3.025	2.780

Table XI. The comparison of RMS and peak values when the mass = (1-20%)MHcar and road class is average($\times 10^{-3}$):

		Front body acceleration	Rear body acceleration	Pitch acceleration	Front body deflection	Rear body deflection
FLC	Peak	18.630	4.131	0.2082	13.660	12.420
	RMS	3.794	0.8362	0.1120	6.346	5.800
BIFC	Peak	2.035	0.3245	0.1194	6.177	4.016
	RMS	0.9034	0.1441	0.0551	3.009	2.109

Table XII. The comparison of RMS and peak values when the mass = (1+20%)MHcar and road class is average($\times 10^{-3}$):

		Front body acceleration	Rear body acceleration	Pitch acceleration	Front body deflection	Rear body deflection
FLC	Peak	34.13	7.541	0.2669	14.541	13.070
	RMS	4.610	1.014	0.1320	6.614	5.957
BIFC	Peak	2.909	0.4646	0.1474	6.4846	5.982
	RMS	1.367	0.2184	0.0649	3.2184	2.872

Table XIII. The comparison of RMS and peak values when the mass = Mcar and road class is poor($\times 10^{-3}$):

		Front body acceleration	Rear body acceleration	Pitch acceleration	Front body deflection	Rear body deflection
FLC	Peak	25.150	5.577	0.3546	19.64	17.540
	RMS	5.270	1.159	0.1542	9.089	8.340
BIFC	Peak	4.259	0.6204	0.1938	9.153	8.421
	RMS	1.560	0.2491	0.0851	4.348	4.008

Table XIV. The comparison of RMS and peak values when mass = (1-20%)MHcar and road class is poor($\times 10^{-3}$):

		Front body acceleration	Rear body acceleration	Pitch acceleration	Front body deflection	Rear body deflection
FLC	Peak	24.340	5.395	0.2944	19.310	15.660
	RMS	4.318	0.9523	0.149	9.098	8.315
BIFC	Peak	2.890	0.4608	0.1690	8.860	9.923
	RMS	1.317	0.2101	0.0802	4.115	4.425

Table XV. The comparison of RMS and peak values when mass = (1+20%)MHcar and road class is poor($\times 10^{-3}$):

		Front body acceleration	Rear body acceleration	Pitch acceleration	Front body deflection	Rear body deflection
FLC	Peak	27.11	6.020	0.3774	19.820	17.670
	RMS	6.705	1.476	0.1575	10.416	9.804
BIFC	Peak	5.113	0.6571	0.2085	11.073	10.190
	RMS	1.979	0.3160	0.0932	4.844	5.572

Table XVI. The comparison of RMS and peak values, K1& K3= (original values \pm 20%) and road class is average

		Front body acceleration $\times 10^{-3}$	Rear body acceleration $\times 10^{-3}$	Pitch acceleration $\times 10^{-3}$
+20%	BIFC	RMS	2.057	0.3282
		Peak	3.911	0.6240
	FLC	RMS	7.113	1.552
		Peak	14.280	3.439
-20%	BIFC	RMS	2.064	2.253
		Peak	5.057	5.136
	FLC	RMS	3.254	3.428
		Peak	1.048	10.040

Table XVII. The comparison of RMS and peak values, K1& K3= (original values+/-20%) and road class is poor

			Front body deflection $\times 10^{-3}$	Rear body deflection $\times 10^{-3}$
+20%	BIFC	RMS	2.138	2.292
		Peak	4.872	4.866
	FLC	RMS	3.368	3.501
		Peak	9.744	9.176
-20%	BIFC	RMS	1.924	0.3071
		Peak	3.805	0.6073
	FLC	RMS	5.809	1.268
		Peak	13.600	2.974

Table XVIII. The crest factors Comparison for average road profile

Crest factor (CF)			
Average Road	Front body acceleration	Rear body acceleration	Pitch acceleration
BIFC	2.137	2.139	1.532
FLC	4.422	4.453	2.236

Table XIX. The crest factors Comparison for poor road profile

Crest factor (CF)			
Poor Road	Front body acceleration	Rear body acceleration	Pitch acceleration
BIFC	2.730	2.491	2.277
FLC	4.772	4.812	2.30

REFERENCES

1. A. Raj, S. Shrivastava, M W Trikande, "Modelling and Analysis of Skyhook and Fuzzy Logic Controls in Semi-Active Suspension System," *IEEE International Conference on Industrial Instrumentation and Control*, 2015, pp. 730 – 734.
2. Y. L. Hu, M. Z. Q. Chen, and Z. S. Hou, "Multiplexed model predictive control for active vehicle suspensions," *Int. J. Control*, vol. 88, no. 2, 2015, pp. 347–363.
3. S. Wen, Michael Z. Q. Chen, Z. Zeng, X. Yu, and T. Huang, "Fuzzy Control for Uncertain Vehicle Active Suspension Systems via Dynamic Sliding-Mode Approach," *IEEE transactions on systems, man, and cybernetics: systems*, 2016, pp.1-9.
4. H. Y. Li, H. H. Liu, H. J. Gao, and P. Shi, "Reliable fuzzy control for active suspension systems with actuator delay and fault," *IEEE Trans. Fuzzy Syst.*, vol. 20, no. 2, 2012, pp. 342–357.
5. H. Y. Li, J. Y. Yu, C. Hilton, and H. H. Liu, "Adaptive sliding-mode control for nonlinear active suspension vehicle systems using T–S fuzzy approach," *IEEE Trans. Ind. Electron.*, vol. 60, no. 8, 2013, pp. 3328–3338.
6. W. C. Sun, H. J. Gao, and O. Kaynak, "Adaptive backstepping control for active suspension systems with hard constraints," *IEEE Trans. Mechatronics*, vol. 18, no. 3, 2013, pp. 1072–1079.
7. W. C. Sun, Z. L. Zhao, and H. J. Gao, "Saturated adaptive robust control for active suspension systems," *IEEE Trans. Ind. Electron.*, vol. 60, no. 9, 2013, pp. 3889–3896.
8. Y. L. Hu, M. Z. Q. Chen, and Z. Shu, "Passive vehicle suspensions employing inerters with multiple performance requirements," *J. Sound Vib.*, vol. 333, no. 8, 2014, pp. 2212–2225.
9. L. S.Louca, "Modal analysis reduction of multi-body systems with generic damping," *Journal of Computational Science*, vol. 5, no. 3, 2014, pp. 415-426.
10. R.N Jazar, "Quarter Car Model," *In: Vehicle Dynamics. Springer*, New York, NY. ISBN 978-1-4614-8543-8., 2014.
11. A. Kulkarni, S. A Ranjha, A. Kapoor, "A quarter-car suspension model for dynamic evaluations of an in-wheel electric vehicle," *Journal of Automobile Engineering*, vol 232, Issue 9, 1139-1148 , 2018.
12. M. Du, F. Zhao, B. Yang, L. Wang, "Terminal sliding mode control for full vehicle active suspension systems," *J. of Mechanical Science and Technology*, vol. 32, no. 6, 2018, pp 2851–2866.
13. P. Senthilkumar, K. Sivakumar, R. Kanagarajan, S. Kuberan, "Fuzzy Control of Active Suspension System Using Full Car Model," *dynamics of mechanical systems, Makanika J*, Vol. 24, 2, 2018, pp. 240-247.
14. B. Chen, C. Lin, X. Liu, and K. Liu, "Observer-based adaptive fuzzy control for a class of nonlinear delayed systems," *IEEE Trans. Syst., Man, Cybern., Syst.*, vol. 46, no. 1, 2016, pp. 27–36.
15. S. Tong, L. Zhang, and Y. Li, "Observed-based adaptive fuzzy decentralized tracking control for switched uncertain nonlinear large-scale systems with dead zones," *IEEE Trans. Syst., Man, Cybern., Syst.*, vol. 46, no. 1, 2016, pp. 37–47.
16. P. Wongl, Z. Xie2, H. Wong, X. Huang," Design of a Fuzzy Preview Active Suspension System for Automobiles," *Proceedings of 2011 International Conference on System Science and Engineering*, China, 2011, pp. 525- 529..
17. N. S. Bhangal and K. Amit Raj, "Fuzzy Control of Vehicle Active Suspension System," *International Journal of Mechanical Engineering and Robotics Research*. vol. 5, no. 2, 2016, pp. 144-148.
18. S. Rajendiran and P. Lakshmi, Simulation of PID and fuzzy logic controller for integrated seat suspension of a quarter car with driver model for different road profiles," *Journal of Mechanical Science and Technology*. Vol. 30(10), 2016, pp. 4565-4570.
19. H. Al-Mutar and T. Y. Abdalla, "Quarter Car Active Suspension System Control using Fuzzy Controller tuned by PSO," *Int. J. of Computer Applications*, vol. 127 – no.2, 2015, pp. 38-43.
20. R. Al-Jarrah and H. Roth,"Developed Blimp Robot Based On Ultrasonic Sensors Using Possibilities Distribution and Fuzzy Logic," *Journal of Automation and Control Engineering*, vol. 1, no. 2, 2013, pp. 1-7.
21. B. Das, M. Maiti,"Fuzzy stochastic inequality and equality possibility constraints and their application in a production-inventory model via optimal control method," *Journal of Computational Science*, vol. 4, issue 5, 2013, pp. 360-369.
22. R. Al-Jarrah, R. Ait Jellal and H. Roth, "Blimp based on Embedded Computer Vision and Fuzzy Control for Following Ground Vehicles," *3rd IFAC Symposium on Telematics Applications, The International Federation of Automatic Control*, 2013, pp. 7-13.
23. Y. Ming Chen, C. Hsueh, V. Wang, T. Wu, "Decision fusion using fuzzy threshold scheme for target detection in sensor networks," *Journal of Computational Science*, vol. 25, 2018, pp. 327-338.
24. P. harliana1, R. Rahim,"Comparative Analysis of Membership Function on Mamdani Fuzzy Inference System for Decision Making," *Int. Conf. on Info. and Comm. Tech.*, Series 930-012029, 2017.



25. O. R. Carvajal, O. Castillo, J. Soria, "Optimization of Membership Function Parameters for Fuzzy Controllers of an Autonomous Mobile Robot Using the Flower Pollination Algorithm," *J. of Automation, Mobile Robotics & Intelligent Systems*, vol. 12, no. 1, 2018, pp.44-49.
26. P. Aimtongkham, T. Nguyen, C. So-In, "Congestion Control and Prediction Schemes Using Fuzzy Logic System with Adaptive Membership Function in Wireless Sensor Networks," *Wireless Comm. and Mobile Computing J.*, vol. 2018, 2019, 19 pages.
27. R. Al-Jarrah, M. Al-Jarrah, H. Roth, "A Novel Edge Detection Algorithm for Mobile Robot Path Planning," *J. of Robotics*, vol. 2018, ID 1969834.
28. R. Darus and N. I. Enzai, "Modeling and control of active suspension system for quarter car model," *International Conference on Science and Social Research*, Malaysia, 2010.
29. R. Al-Jarrah and H. Roth, "Design Blimp Robot Based on Embedded system and software architecture with high level communication and fuzzy logic," *the 9th International Symposium on Mechatronics and its Applications*, Jordan, 2013.
30. Q. Liang, and J. Mendel, "Interval type-2 fuzzy logic systems: theory and design," *IEEE Trans. Fuzzy Systems*, vol. 8, no.5, 2000, pp. 535-550.
31. J. Cao, H. Liu, P. Li, and D. Brown, "Adaptive fuzzy logic controller for vehicle active suspensions with interval type-2 fuzzy membership functions," *the IEEE International Conference on Fuzzy systems*. Hong Kong, 2008, pp.83-89.
32. Yi-Hsun Lo, Rui-Peng Chen, Lian-Wang Lee, I-Hsum Li, and Ya-Dung Pan, Design and Implementation of a Interval Type-2 Adaptive Fuzzy Controller for a Novel Pneumatic active Suspension System, *17th International Symposium on Advanced Intelligent Systems (ISIS)*, pp. 801-805, 2016.
33. Sorina Costache, Litescu Vaisagh, Viswanathan Heiko, Aydt Alois Knoll, The Effect of Information Uncertainty in Road Transportation Systems, *Journal of Computational Science*, Vol. 16, pp. 170-176, 2016.
34. C. Chen, G. Rigatos, D. Dong, and J. Lam, "Partial Feedback Control of Quantum Systems Using Probabilistic Fuzzy Estimator," *Proceedings of the 48th IEEE Conference on Decision and Control*, 20019, pp. 3805 - 3810.
35. R. Al-Jarrah, A. Shahzad and H. Roth, "Path Planning and Motion Coordination for Multi-Robots System Using Probabilistic Neuro-Fuzzy," *Elsevier conference paper archive, IFAC-Papers On Line*, 2015, pp. 046-051.
36. ISO, reporting vehicle road surface irregularities, Technical report, ISO, ISO/TC108/SC2/WG4 N57, 1982.
37. D.T. Hamid, "Automobile passenger comfort assured through lqg/lqr active suspension," *J. of Vibration and Control*, vol. 3, 1997, pp. 1-19.
38. ISO 2631-1: 1997. Mechanical vibrations and shock – evaluation of human exposure to whole-body vibration – part 1: general requirements, 1997 (*International Organization for Standardization*, Geneva).
39. F. Tyan , Y. Hong, S-H Tu and W. S. Jeng, "Generation of Random Road Profiles," *The Journal of the Chinese Society of Mechanical Engineers*, 2009, pp. 1373-1378.
40. N.J. Mansfield, human response to vibration, by CRC Press LLC, Boca Raton, 2005.



Hitham Tlilan, earned his Ph.D degree in the area of Solids and Fracture Mechanics from the Chiba University, Chiba, Japan in 2005. He is an Associate Professor in the Department of Mechanical Engineering at Hashemite University, Zarqa, Jordan. He has published papers in the areas of Mechanical Engineering; Strength and fracture mechanics of notched bars. Strain and Stress-concentration factors under different types of loading, Linear and Non-linear dynamics. Mechanical Vibrations, Automatic control, Thermo-Fluids Mechanics, Water, Energy, and Environment. He advised more than 15 graduate students and undergraduate. He attended/organized several international conferences/symposia and presented research papers. He has over 13 years of teaching and research experience.



Ayat Al-Jarrah, She is a full time lecturer at mechatronics engineering department, Hashemite University, Jordan. She graduated with Bachelor and Master degree from Jordan University of Science and Technology, Jordan in 2009 and 2012, respectively. Her research interests are Automatic Control, Dynamics systems, Vibrations, Mechanical Design, Modeling and Simulation, Design of Mechatronics System. She is a member of Jordanian Engineering Association.

AUTHORS PROFILE



Rami AL-Jarrah, He is Assistant Professor at mechanical engineering department, Hashemite University, Jordan. He graduated with Bachelor and Master degree from Jordan University of Science and Technology, Jordan in 2002 and 2004, respectively. He graduated with Dr.-Ing. of Robotics and Control Systems from Regelungs-und-Steuerungstechnik Institute, Siegen University, Germany 2015. His research interests are Mechanical Design and Modeling, Fuzzy sets, Fuzzy Control, Control Systems, Mobile Robots Navigations , and Optimizations, and Wireless Sensor Networks.. He has a membership of the Jordanian Engineering Association and has been actively participated in several international research conferences since 2013. He has various publications including ISI and Scopus from the period 2013 to 2019. He has reviewed lots of research papers for international journals and has been acknowledged for the services.